NASA Technical Memorandum 104431

Tuned Optimization of Extended Reacting Acoustic Liners

Kenneth J. Baumeister
Lewis Research Center
Cleveland, Ohio

Prepared for the
1991 Winter Annual Meeting of the American Society of Mechanical Engineers
Atlanta, Georgia, December 1-6, 1991

NASA

TUNED OPTIMIZATION OF EXTENDED REACTING ACOUSTIC LINERS

Kenneth J. Baumeister
National Aeronautics and Space Administration
Lewis Research Center
Cleveland, Ohio 44135

ABSTRACT

A finite-element Galerkin formulation has been employed to study the optimum attenuation and reflection characteristics of acoustic waves propagating in two-dimensional straight ducts with extended reacting absorbing walls without a mean flow. The reflection and transmission of acoustic energy at the entrance and the exit of the duct were determined by coupling the finite-element solutions in the absorbing portion of the duct to the eigenfunctions of an infinite, uniform, hard wall duct. In the frequency range where the duct height and acoustic wave length are nearly equal, power attenuation contours were examined to determine conditions for minimizing acoustic transmission through the duct. The extended reacting liners were found to significantly minimize the transmission of acoustic energy when the liner wall properties were tuned to maximize the reflective characteristics of the duct rather than to increase absorption in the liner. Thus, extended reacting wall liner properties can be theoretically chosen to yield large impedance mismatches in an open straight duct.

NOMENCLATURE

b' characteristic duct height

b_a dimensionless entrance height b_a'/b'

c_o' adiabatic speed of sound

E acoustic power

f dimensionless frequency, Eq. (3)

j $\sqrt{-1}$

L dimensionless length (see Fig. 2), L'/b'

$\bar{n}$ outward unit normal

P dimensionless acoustic pressure, $P'(x,y,t)/\rho_{oa}' c_{oa}'^2$

p dimensionless acoustic pressure, $P(x,y,t)/e^{j\omega t}$

t dimensionless time, $t'c_{oa}'/b_a'$

x dimensionless axial distance, x'/b_a'

y dimensionless transverse distance, y'/b_a'

ε dimensionless complex acoustic permittivity

μ dimensionless complex acoustic permeability

ρ_o dimensionless density, ρ_c'/ρ_{oa}'

ω' angular velocity, $2\pi f'$

ω dimensionless angular velocity, $\omega'b_a'/c_o'$

Subscripts:

a inlet duct condition

o ambient condition

x x component

y y component

Superscript:

$'$ dimensional quantity

R real part

I imaginary part

INTRODUCTION

In sound absorbing ducts without a mean flow, the absorptive characteristics of lined straight ducts have been modeled by applying the classical admittance boundary conditions at the duct walls. Admittance or impedance type boundary conditions apply to locally reacting liners. In a locally reacting liner, such as a Helmholtz resonator array behind a perforated plate,

the sound energy interacts normally to the liner and depends only on the local value of acoustic pressure in the adjacent acoustic field. Optimizing locally reacting wall absorber for maximum attenuation is an important part of the design of an acoustic duct suppressor. In duct acoustics employing local impedance boundary conditions, the maximum possible attenuation occurs at the so-called optimum impedance. For a particular acoustic mode or more generally for modes with common cut-off ratios, the optimum impedance can be determined analytically from semi-infinite duct theory using a single soft-wall mode (Rice, 1979). Unruh (1976) has determined the optimum impedance for finite length liners.

In contrast, the extended reaction liner permits wave propagation in the axial direction through the liner, as shown in Fig. 1, and its attenuation characteristics depends on the entire acoustic field. Fiber-glass or Kevlar would be some typical bulk absorber material. Baumeister and Dahl (1987 and 1989) developed a finite element model to study wave propagation in bulk materials as well as in any heterogeneous medium. The absorptive characteristics of the bulk materials, acoustic permittivity and permeability used in those studies relied on the semi-theoretical development presented by Hersh (1980). The theory and property formulas were validated by a number of experiments. Again, optimizing an extended reacting wall absorber for maximum attenuation plays an important part of the design of an acoustic duct suppressor. For plane wave propagation, Baumeister (1989) has examined a range of wall properties associated with optimizing absorption in an extended reacting liner.

In the present paper, a finite element model will be used to continue the study of the optimum wave attenuation in straight ducts with extended reacting absorbing walls. The present investigation will focus on the optimal properties of extended reaction wall liners of straight ducts over a larger range of the duct wall properties than has previously been considered. In the frequency range where the duct height and acoustic wave length are nearly equal, power attenuation contours will be examined to determine conditions for maximum acoustic power absorption.

GEOMETRIC MODEL

Consider the idealized acoustic duct shown in Fig. 2 which can be used to simulate acoustic wave propagation in a rectangular two dimensional straight duct in the absence of flow. The interior passage is assumed to contain air while an acoustic bulk absorber is mounted in the cavity above and below the duct in the central portion. The dimensionless duct coordinates are defined as

$$Y = \frac{y'}{b'_a} \qquad x = \frac{x'}{b'_a} \qquad L = \frac{L'}{b'_a} \qquad (1)$$

and b'_a is the dimensional height of the straight duct leading into the finite element region. Absorption of the incoming wave's energy takes place in the finite element region embedded in the wall absorber. In the foregoing equations, the prime is used to denote a dimensional quantity and the unprimed symbols define a dimensionless quantity. This convention will be used throughout this paper. These and all other symbols used in the paper are defined in the nomenclature.

Some sort of acoustic pressure disturbance is assumed to generate a harmonic pressure field at minus infinity in the entrance duct. This field will propagate down the duct and act as the input driving bound-

ary condition for the problem. A positive going acoustic wave of known magnitude is assumed at the entrance (x = 0.0) of the finite element portion of the duct. The pressure wave may be plane or have significant transverse y pressure variations. The present paper will focus on the interaction of plane propagating acoustic waves with the extended reaction absorbing materials.

In the uniform, infinitely long entrance and exit duct regions with perfectly hard walls, the exact solution of the governing differential equations can be easily written in terms of the duct modes (Astley and Eversman 1981); thus, simple analytical expressions can be employed to describe the pressure field in these regions. In the central region which includes both the duct and the fibrous region, the finite element analysis is employed to determine the pressure field.

The assumed known pressure waves propagating down the hard wall entrance duct are partially reflected, transmitted and absorbed by the nonuniform segment of the duct containing the acoustic absorber. Pressure mode reflection at the inlet to the absorbing region and transmission at the outlet of the absorbing region are determined by matching the finite element solution in the interior of the central region to the known analytical eigenfunction expansions in the uniform inlet and exit ducts. This permits a multimodal representation accounting for reflection and mode conversion by the nonuniform absorbing section (Astley and Eversman 1981). This approach has been found to accurately model reflection and transmission coefficients (Baumeister et al. 1983).

GOVERNING EQUATION AND BOUNDARY CONDITIONS

The acoustic propagation through the two-dimensional Cartesian duct and absorber regions in Fig. 2 can be modeled by solutions of the continuity, momentum, and state linearized gas dynamic equations in the absence of flow. As developed by Baumeister and Dahl (1987), for harmonic pressure propagation in a heterogeneous bulk material, the equations of state, continuity, and conservation of momentum were combined to yield the following wave equation in dimensionless form:

$$\frac{\partial}{\partial y}\left(\frac{1}{\epsilon_y}\frac{\partial p}{\partial y}\right) + \frac{\partial}{\partial x}\left(\frac{1}{\epsilon_x}\frac{\partial p}{\partial x}\right) + \omega^2\mu p = 0 \qquad (2)$$

where the dimensionless frequency associated with this Helmholtz like equation is defined as:

$$f = \frac{b'_a f'}{c'} \qquad \omega = 2\pi f \qquad (3)$$

and $\epsilon_x = \epsilon_y = \epsilon$.

The relationship between acoustic "permittivity" ϵ and acoustic "permeability" μ and the physical properties of the medium is complicated. For propagation in air, ϵ equals the fluid density and μ is the inverse of the product of density and the speed of sound squared. For bulk absorbers, Baumeister and Dahl (1987, Eqs. (25) to (27)) employed Hersh's model (1980) in explicitly relating ϵ and μ to the porosity, a viscous loss coefficient, a heat transfer parameter and an effective speed of sound of the medium. Briefly, for bulk absorbers, the real part of ϵ related to fluid density while its complex part is proportional to a viscous loss coefficient. The μ term is inversely proportional to fluid density and the effective speed of sound which depends on the heat transfer character-

2

of sound which depends on the heat transfer character-istics of the media. The formula for ϵ and μ are given by Eqs. (5) and (7) of Baumeister and Dahl (1987). Morse and Ingard (1968, p. 253) also developed more general parameters for describing propagation in porous media for which ϵ and μ can be related.

In the present paper, the parameters ϵ and μ will be treated as mathematical quantities independent of property correlations. In particular, the values of ϵ and μ associated with the optimum absorption properties will be examined. Both these quantities are complex with the imaginary parts associated with dissipative losses.

At the hard walls shown by the dark thick lines in Fig. 2, the acoustic velocity normal to the wall is zero. Again, using the momentum equations to relate the acoustic velocity to the pressure fields requires

$$\nabla p \cdot \bar{n} = 0 \tag{4}$$

In addition, recall that a modal solution (Morse and Ingard 1968, p. 504) is used to represent the pressure in the semi-infinite, hard wall entrance and exit regions while a finite element solution is used to generate the solution in the absorbing portion of the duct. Consequently, both pressure and velocity conti-nuity are required of the modal and finite element solutions at the entrance and exit interfaces separat-ing the finite element and modal regions. This is easily enforced as discussed by Astley and Eversman (1981).

Finally, it is not necessary to employ any inter-facial boundary condition inside the finite element region. For example the thin black line in Fig. 2 separating the air duct from the absorber region requires no special consideration. The heterogeneous form of the wave equation, Eq. (2), automatically han-dles the change in properties.

FINITE ELEMENT THEORY

In the central portion of the duct containing the absorber region, the continuous domain is first divided into a number of discrete triangular areas defined by the corner nodal points, as shown in Fig. 2. The nodal values of $p_i(x_i, y_i)$ are determined by the method of weighted residuals. The finite element aspects of converting Eq. (2) and the boundary conditions into an appropriate set of global difference equations can be found in text books (Burnett 1987) or more explicitly in the paper by Baumeister (1986) and for conciseness will not be presented herein.

RESULTS AND COMPARISONS

A number of sample calculations are now presented to illustrate the use of the finite element theory in minimizing the transmission of the input acoustic sig-nal through a straight duct with bulk absorbers lining the top and bottom walls over a length L. Plots of the power attenuation and reflection contours are used to display the wall properties associated with maximum (optimum) signal attenuation. For a typical straight duct, the grid generation package generates the geome-tries and the linear triangular finite element grid shown in Fig. 2. Calculations were performed with varying grid size to check for convergence of the results. In all the calculations to follow, an absorber of dimensionless length 1.0 and dimensionless thickness of 0.1 has been placed above and below the ducts. The duct height was a dimensionless 1.0 and the

forcing dimensionless acoustic frequency f given by Eq. (3) had a value of unity.

Case 1 - Resistive Dissipation

Consider a plane acoustic wave propagating down a straight duct with a bulk absorber mounted along the walls, as shown in the schematic of Fig. 2. The acoustic attenuation for a fixed value of wall proper-ties was first calculated. Then, by an iteration pro-cess, the local attenuation contours were determined. For an initial assumed ϵ value, the μ plane was searched to find the optimum μ_{opt} which yielded maxi-mum signal attenuation. Next, holding this μ_{opt} fixed, the ϵ plane was searched to find the optimum ϵ_{opt}. This process was repeated now holding ϵ_{opt} fixed and finding a new value of μ_{opt}, and so forth. The final iteration on μ (holding ϵ fixed) for maxi-mum attenuation produced a value of 2.0 + i 2.0. Thus, a four parameter optimization has been performed in a series of two-dimensional optimization processes.

Figure 3 illustrates the characteristic attenua-tion contours as a function of wall properties. In this case, two components of wall material, acoustic permittivity ϵ real and imaginary parts, are used as the abscissa and ordinate to define the wall character-istics with a fixed value of acoustic permeability μ of 2.0 - i 2.0 as calculated by the previous iteration. In the final iteration for the contour plots displayed in Fig. 3, over 1600 separate decibel calculations were performed with increments of 0.5 of the real and imagi-nary values of ϵ throughout the ϵ plane.

The decibel contours in Fig. 3 have been normal-ized between 0 and 1 by the simple expression:

$$\text{Contour level} \sim \frac{|dB| - |dB_{min}|}{|dB_{max}| - |dB_{min}|} \tag{5}$$

The maximum attenuation of the incoming wave is 3.341 dB associated with the local optimum point dis-played in Fig. 3 and as listed in the figure. Because of the high density of the remaining contour plots, the decibel levels of the contours will not be displayed but only the decibel value of the optimum and its coor-dinates will be listed.

For locally reacting liners, the global optimum wall properties are usually represented by the peak contours with a well defined maximum inclosed in the smallest circle as shown in the insert plot of Fig. 3. However, in Fig. 3 the center of the circular local peak appears to the left of the abscissa. This local optimum wall value associated with maximum signal reduction is seen in Fig. 3 to occur at a ϵ of 1.0 - i 5.0 with μ equal to 2.0 - i 2.0. The magni-tude of the imaginary part of ϵ is shown negative in Fig. 3. A number of different starting values of the permeability failed to shift the expected peak on to the plot.

For the same geometry as considered in Fig. 3, the sensitivity of the initial starting material value of ϵ or μ on the contours was examined and found to be quite significant. The local optimum properties can vary depending in the initial starting value of μ used in the optimum search. As another example (not shown in a figure), with μ equal to 4.1 - i 0.0 as the starting point, the local optimum value of ϵ shifted to 1 - i 10.00 with μ remaining at 4.1 - i 0.0. In this new case, the attenuation was a significantly higher 7.465 dB.

The relatively small set of calculations performed here do not guarantee that a global optimum has been

found in the four-dimensional property parameter space (real and imaginary parts of ε and μ). However, they do indicate trends. A series of additional numerical calculations has shown that any combination of material properties with approximately the same ratio of (μ/ε) will have yield similar values of the maximum attenuation. As commonly used in electromagnetic theory, the square root of μ/ε can be defined as an intrinsic impedance of the wall. For Fig. 3 the ratio of μ/ε at the local optimum was 0.461 + i 0.308. In the other example, with μ equal to 4.1 -i 0.0 as the starting point, the ratio of μ/ε changed to 0.0406 + i 0.406 and the attenuation was significantly higher.

Case 2 - Impedance Mismatch

In contrast to the circular like optimum shown by the insert in Fig. 3, observe that for bulk absorbers the contour lines split apart in the lower portion of Fig. 3 rather than form closed rings. This suggests that other local optimums might exist for other values of the acoustic wall material properties that have been missed in the previous searches. To further explore these regions, the next optimum search was initiated with many different starting values. With a starting value of μ equal to 1.0 -i 0.0, the optimum value of ε was found (after a series of iterations in ε and μ space) to be 6.0 - i 0.0 as shown in Fig. 4 and the local optimum attenuation was 7.994 dB. Surprisingly, both ε and μ have real values, which indicate that no absorption occurred from resistive effects in the wall material. Rather, the attenuation in the duct was a result of the wave's energy being reflected back down the duct, as will be shown shortly.

The next iteration sequence was started with a much larger value of μ equal to 14.0 - i 0.0 and the results shown in Figs. 5(a) and 5(b) with contour plots for both permittivity and permeability. The local optimum now occurs at ε of 3.0 - i 0.0. Again since the imaginary part is zero, the attenuation must occur by wave reflection. For this case, the local optimum attenuation was 18.472 db which is an unexpected significant increase in the attenuation characteristics of the duct beyond the simple dissipative effects of the liner. The reflective attenuation contours for the same properties are also displayed in Fig. 6. At ε equals 3.0 - i 0.0, the reflective attenuation is at a minimum value of 0.0625 which implies from Eq. (4) that nearly all the signal is reflected back down the duct.

It is highly unlikely that a material structure could be devised such that its effective properties of ε and μ reached this optimum attenuation point. The porosity would have to be low (0.33) to obtain an ε of 3.0 which is usually associated with viscous material (Zwikker and Kosten, 1949, p. 77). A high value of μ requires a low effective speed of sound. Such low values have only been seen in two phase mixtures like air and water. On the other hand, in the analogous problem of electromagnetic propagation in ducts for which this code was developed, such material structures might easily be manufactured.

CONCLUDING REMARKS

A finite-element Galerkin formulation was used to study optimum acoustic wave attenuation in two-dimensional straight ducts with extended reaction absorbing walls. Optimum properties to maximize wall

absorption were also examined. Designing the acoustic absorber for wave reflection or impedance mismatch yield significantly higher absorption of the incoming sound wave than conventional dissipation in the liner.

The primary aim of the present paper has been to present a new theoretical optimum concept in bulk liner design. However, from a practical point of view, the board band nature of such a liner, it possible construction, and a correlation between ε and μ have not been addressed.

REFERENCES

Astley, R.J. and Eversman, W., 1981, "Acoustic Transmission in Non-uniform Ducts with Mean Flow, Part II: The Finite Element Method," Journal of Sound and Vibration, Vol. 74, pp. 103-121.

Baumeister, K.J., 1986, "Finite Element Analysis of electromagnetic propagation in an absorbing wave guide," NASA TM-88866.

Baumeister, K.J., 1989, "Acoustic Propagation in Curved Ducts With Extended Reacting Wall Treatment," ASME NCA-Vol. 7, Analysis Techniques in Acoustics, H.K. Hsu and R.F. Rettie, eds., ASME, pp. 1-11.

Baumeister, K.J. and Dahl, M.D., 1987, "A Finite Element Model for Wave Propagation in an Inhomogeneous Material Including Experimental Validation," AIAA Paper 87-2741 (also, NASA TM-100149).

Baumeister, K.J. and Dahl, M.D., 1989, "Acoustic Wave Propagation in Heterogeneous Structures Including Experimental Validation," AIAA Paper 89-1044. (Also, NASA TM-101486.)

Baumeister, K.J., Eversman, W., Astley, R.J., and White, J.W., 1983, "Acoustics in Variable Area Duct: Finite Element and Finite Difference Comparisons to Experiment," AIAA Journal, Vol. 21, No. 2, pp. 193-199.

Baumeister, K.J. and Horowitz, S.J., 1984, "Finite Element-Integral Acoustic Simulation of JT15D Turbofan Engine," Journal of Vibration, Acoustics, Stress, and Reliability in Design, Vol. 106, No. 3, pp. 405-413.

Burnett, D.S., 1987, Finite Element Analysis, Addison-Wesley Publishing Company, Reading, MA.

Hersh, A.S. and Walker, B., 1980, "Acoustic Behavior of Fibrous Bulk Materials," AIAA Paper 80-0986.

Morse, P.M. and Ingard, K.U., 1968, Theoretical Acoustics, McGraw-Hill, New York.

Rice, E.J., 1979, "Optimum Wall Impedance for Spinning Modes - A Correlation With Mode Cutoff Ratio," Journal of Aircraft, Vol. 16, No. 5, pp. 336-343.

Unruh, J.F., 1976, "Finite Length Tuning for Low Frequency Lining Design, Journal of Sound and Vibration, Vol. 45, No. 1, pp. 5-14.

Zwikker, C. and Kosten, C.W., 1949, Sound Absorbing Materials, Elsevier Publishing Co., New York.
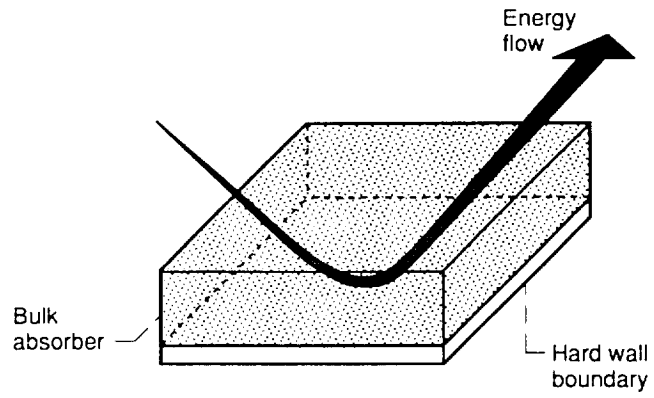
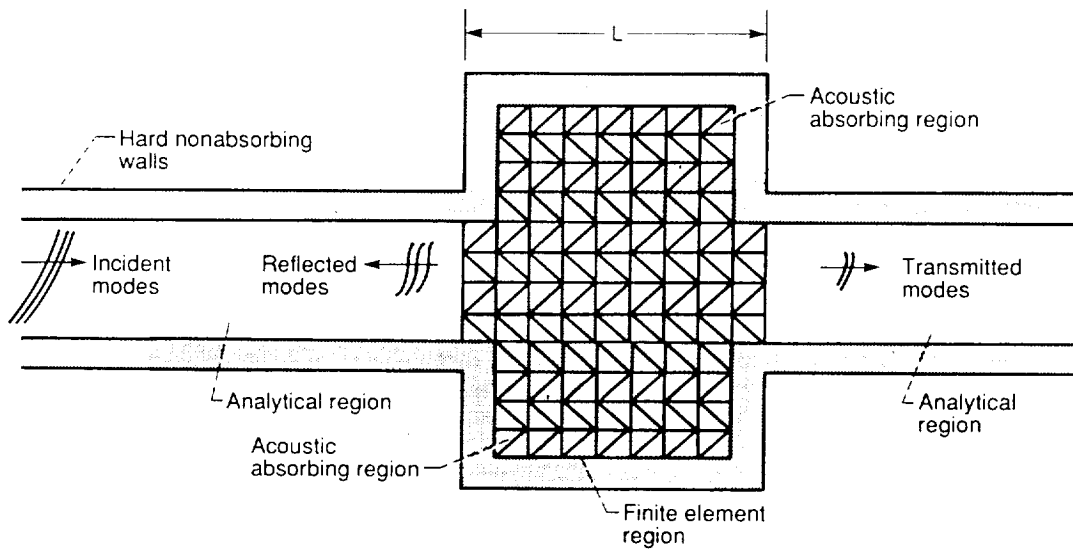Figure 1.—Extended reacting liner and boundary condition.

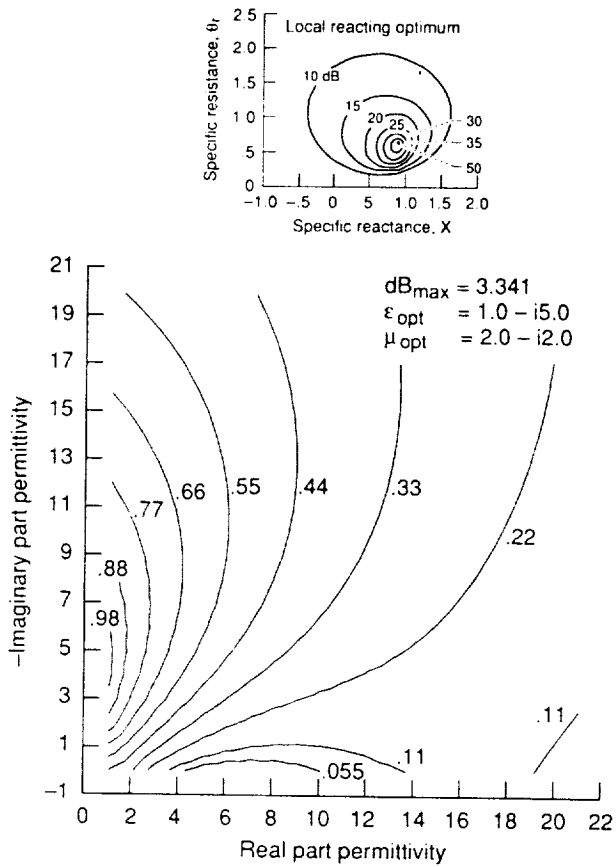Figure 2.—Two dimensional duct finite element model. (Not to scale).

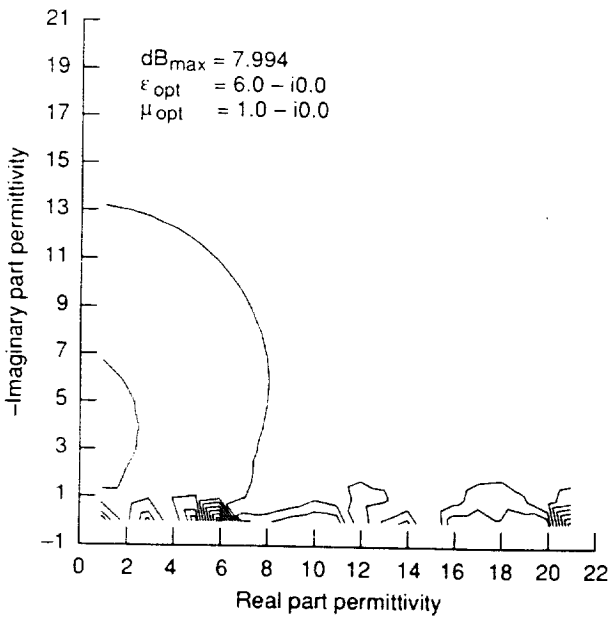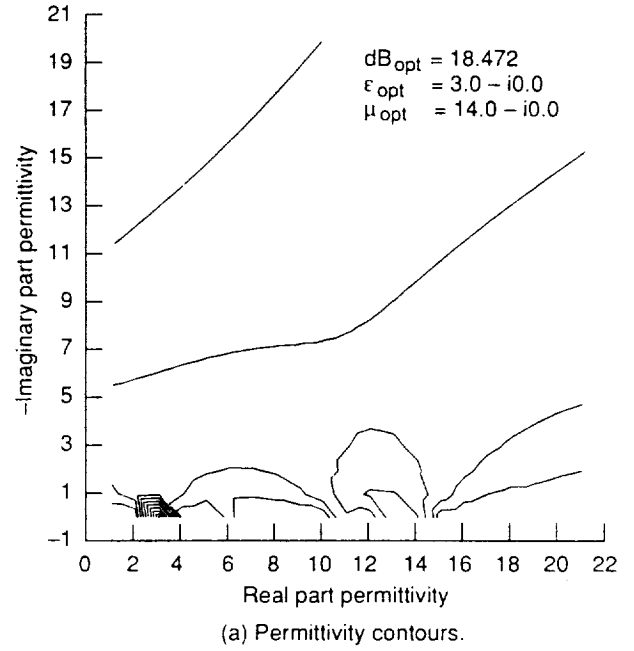Figure 3.—Normalized acoustic attenuation contours for straight duct with bulk absorber.

(a) Permittivity contours.

Figure 4.—Acoustic attenuation contours for straight duct - initial iteration.
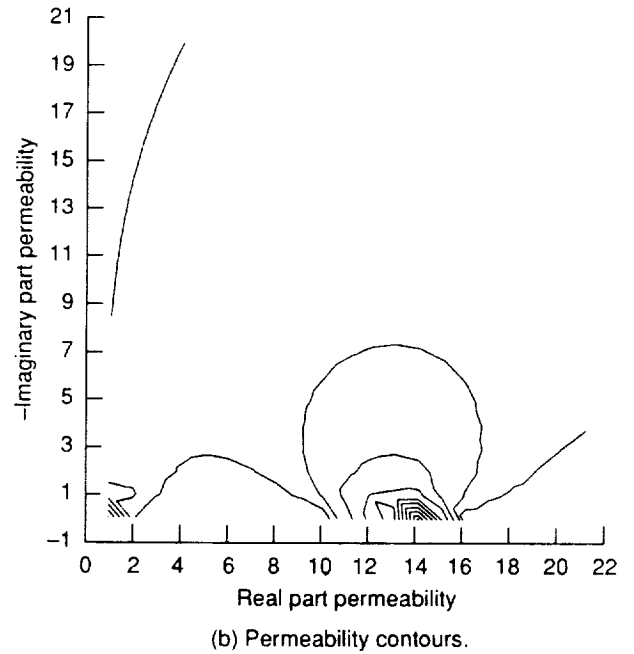

(b) Permeability contours.

Figure 5.—Acoustic attenuation contours for straight duct - final iteration.

6

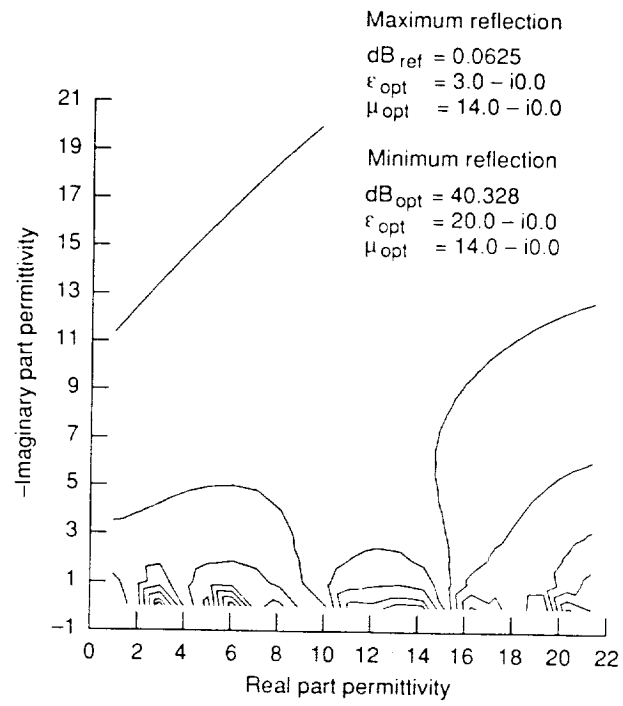Figure 6.—Acoustic reflection contours for straight duct - final iteration.

Report Documentation Page

1. Report No. NASA TM-104431	2. Government Accession No.	3. Recipient's Catalog No.

4. Title and Subtitle

Tuned Optimization of Extended Reacting Acoustic Liners

5. Report Date

6. Performing Organization Code

7. Author(s)

Kenneth J. Baumeister

8. Performing Organization Report No.

E-6265

10. Work Unit No.

505-62-52

9. Performing Organization Name and Address

National Aeronautics and Space Administration
Lewis Research Center
Cleveland, Ohio 44135-3191

11. Contract or Grant No.

13. Type of Report and Period Covered

Technical Memorandum

12. Sponsoring Agency Name and Address

National Aeronautics and Space Administration
Washington, D.C. 20546-0001

14. Sponsoring Agency Code

15. Supplementary Notes

Prepared for the 1991 Winter Annual Meeting of the American Society of Mechanical Engineers, Atlanta, Georgia, December 1-6, 1991. Responsible person, Kenneth J. Baumeister, (216) 433-5886.

16. Abstract

A finite-element Galerkin formulation has been employed to study the optimum attenuation and reflection characteristics of acoustic waves propagating in two-dimensional straight ducts with extended reacting absorbing walls without a mean flow. The reflection and transmission of acoustic energy at the entrance and the exit of the duct were determined by coupling the finite-element solutions in the absorbing portion of the duct to the eigenfunctions of an infinite, uniform, hard wall duct. In the frequency range where the duct height and acoustic wave length are nearly equal, power attenuation contours were examined to determine conditions for minimizing acoustic transmission through the duct. The extended reacting liners were found to significantly minimize the transmission of acoustic energy when the liner wall properties were tuned to maximize the reflective characteristics of the duct rather than to increase absorption in the liner. Thus, extended reacting wall liner properties can be theoretically chosen to yield large impedance mismatches in an open straight duct.

17. Key Words (Suggested by Author(s))

Finite element method
Acoustic attenuator
Acoustic properties

18. Distribution Statement

Unclassified - Unlimited
Subject Category 71

19. Security Classif. (of the report) Unclassified	20. Security Classif. (of this page) Unclassified	21. No. of pages 8	22. Price* A02